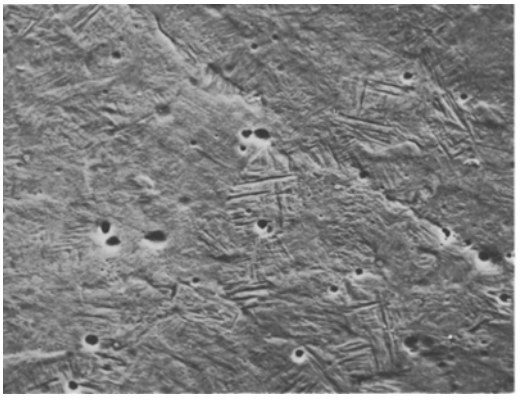

Figure 2 Scanning electron micrograph of the interface between the welded parts. × 865.

microprobe analysis gave no segregation of iron, chromium and tin in the welded zone.

As a result of this investigation the microstructure in a resistance (projection) welded of zircaloy 4 seems a martensitic-type structure or a very fine widmanstätten structure (with a plate thickness less than 0.5 μm). Bodmer *et al.* [6] reported the presence of a martensitic structure in fast-cooled electron-beam welded zircaloy 2. A careful study must be continued.

References

1. J. A. GREENWOOD, *Brit. Weld. J.* 8 (1961) 316.
2. S. DE BURBURE, *Weld. J.* 57 (1970) 322.
3. R. A. HOLT, *J. Nuclear Mater.* 35 (1970) 322.
4. *Idem, ibid* 47 (1973) 262.
5. O. T. WOO and K. TANGRI, *ibid* 79 (1979) 82.
6. E. BODMER, J. J. CHÈNE, R. O. ERIKSON and R. FERRARINI, Proceedings of the 3rd International Conference on the Peaceful Uses of Atomic Energy, Geneva, Set 1964, United Nations (United Nations Publications, New York, 1965) Vol. 9 p. 173.

Received 3 August
and accepted 20 September 1979

A. M. OLMEDO
Comisión Nacional de Energía Atómica,
Dpto INEND,
Argentina

Planar interfaces in Cr_2O_3-doped calcium aluminoferrite

Incorporation of chromium ions into the crystal structure of calcium aluminoferrite increases the early hydraulic activity of the respective ferrite phase. This has been observed by Sakurai *et al.* [1] who consider the beneficial effect of chromium to be associated with the semiconductivity phenomena. When investigating the Ca_3SiO_5–Cr_2O_3 solid solutions the same authors concluded that chromium-induced screw dislocations act as starting points of the hydration process. The same has been proposed for hydration of Cr_2O_3-doped aluminoferrites, although in this case experimental evidence of the presence of screw dislocations has not been given.

In order to verify whether the crystal imperfections in Cr_2O_3-doped calcium aluminoferrite are of an analogous type and density as in the case of Ca_3SiO_5-solid solution, we have examined a sample of Cr_2O_3-doped calcium aluminoferrite by transmission electron microscopy. The sample was synthesized as described by Sakurai *et al.* [1]; for preparation of the raw mixture containing 47% CaO, 29% Fe_2O_3, 18.5% Al_2O_3 and 5.5% Cr_2O_3, analytical grade chemicals were used. The mixture was fired for 2 h at 1300° C and cooled at a rate of 50° C h^{-1}. The product of synthesis was checked by X-ray diffraction; the diffraction pattern showed no other reflections than those ascribable to calcium aluminoferrite. The average unit cell parameters are: $a = 5.36$ Å, $b = 14.50$ Å and $c = 5.58$ Å, which are in general agreement with the literature data for $Ca_2Fe_{0.5}Al_{0.5}O_5$ [2–4].

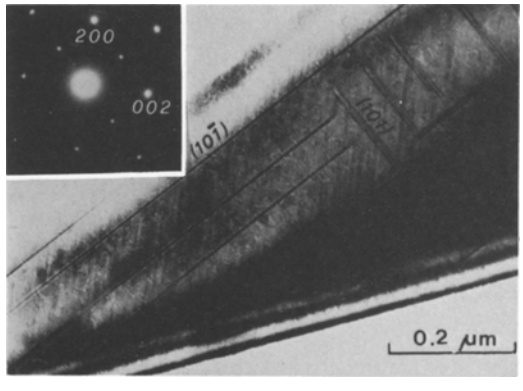

Figure 1 TEM and $h\,0\,l$ electron diffraction pattern of Cr_2O_3-doped calcium aluminoferrite.

0022–2461/80/041051–04$02.40/0

The TEM specimens were prepared by grinding the sample in ethanol and spraying the dilute suspension onto carbon-coated specimen grids with a thin evaporated layer of aluminium serving as an internal diffraction standard. An electron microscope (Philips EM 300) operating at 100 kV was used. Fig. 1 is a typical example of the micrographs obtained. Instead of the expected linear defects, planar interfaces parallel to (1 0 1) and (1 0 $\bar{1}$) are visible in these micrographs. Interfaces parallel to (0 0 1) exhibiting weak contrast and only about 100 Å apart are also visible. None of these features were observed in the simultaneously prepared calcium aluminoferrite without Cr_2O_3 addition.

At a first glance the contrast at (1 0 1) and (1 0 $\bar{1}$) interfaces could be associated with stacking faults or antiphase boundaries. This is supported by the observed fringe patterns, symmetrical in the bright field and asymmetrical in the dark field [5]. Diffraction contrast analysis involving the condition $2\pi\mathbf{g} \cdot \mathbf{R} = 0$ or $2\pi n$ (n = integer) is illustrated in Fig. 2 where three dark-field images obtained with different operating reflections are shown. A survey of contrast visibility with $h\,0\,l$ and $0\,k\,0$ reflections is given in Table I. Invisibility of the (1 0 1) interface when using $h\,0\,l$ reflections indicates that the displacement vector **R** lies in the respective plane. The visibility of these interfaces with higher order reflections of the $h\,0\,l$ type having h equal to l shows that the magnitude of **R** must be small, i.e. that its x- and z-components are most likely smaller than $\frac{1}{6}$. Since $0\,k\,0$ reflections are extinguished due to the space group symmetry, they could not be included in diffraction contrast analysis, so the y-components of **R** may equal 0 or $\frac{1}{2}$. An analogous consideration was applied for the (1 0 $\bar{1}$) and (0 0 1) interfaces. This yields the following possible translation vectors **R** for various interfaces:

(1 0 $\bar{1}$): $\mathbf{R}_1 = [p\,0\,p]$ or $[p\,\frac{1}{2}\,p], p < \frac{1}{6}$;

(1 0 1): $\mathbf{R}_2 = [p\,0\,\bar{p}]$ or $[p\,\frac{1}{2}\,\bar{p}], p < \frac{1}{6}$;

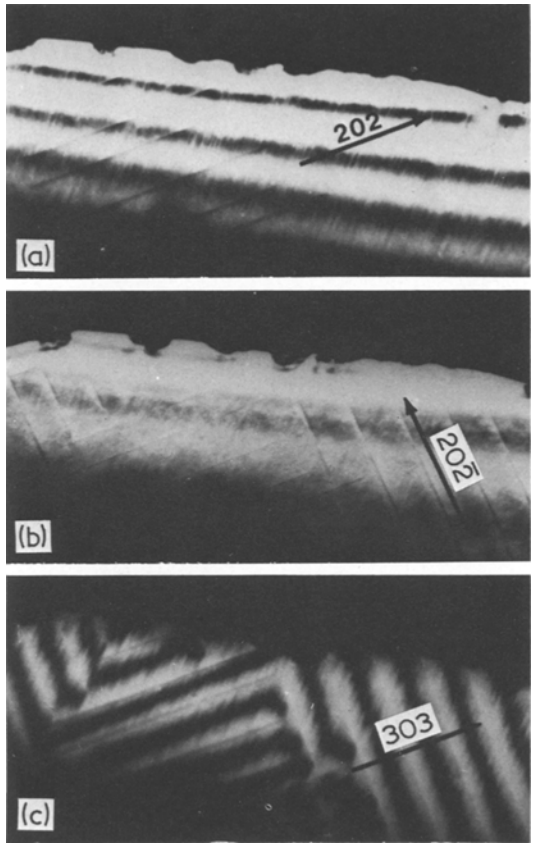

Figure 2 Characteristic dark-field micrographs used in the diffraction contrast analysis.

(0 0 1): $\mathbf{R}_3 = [p\,0\,\frac{1}{2}]$ or $[p\,\frac{1}{2}\,\frac{1}{2}], \frac{1}{2} > p > \frac{1}{2} - \frac{1}{6}$.

It should be noted that the features of the dark-field images obtained with a 3 0 3 reflection (Fig. 2c), and also with some other weak reflections, are not typical for translation faults. The observed change of contrast between adjacent (1 0 1) or (1 0 $\bar{1}$) interfaces must be associated with the differences in the respective structure amplitudes. The different structure amplitudes in the adjacent regions are characteristic for coherent precipitates or exsolution lamellae [5], and this indicates that in the case of Cr_2O_3-doped

TABLE I Visibility of Interfaces as a Function of Operating Reflection g (V: Visible; I: Invisible)

Interface	g						
	200	002	202	$20\bar{2}$	303	$30\bar{3}$	$0k0$ ($k = 2n$)
(1 0 $\underline{1}$)	V	V	I	V	I	V	I
(1 0 1)	V	V	V	I	V	I	I
(0 0 1)	V	I	V	V	V	V	I

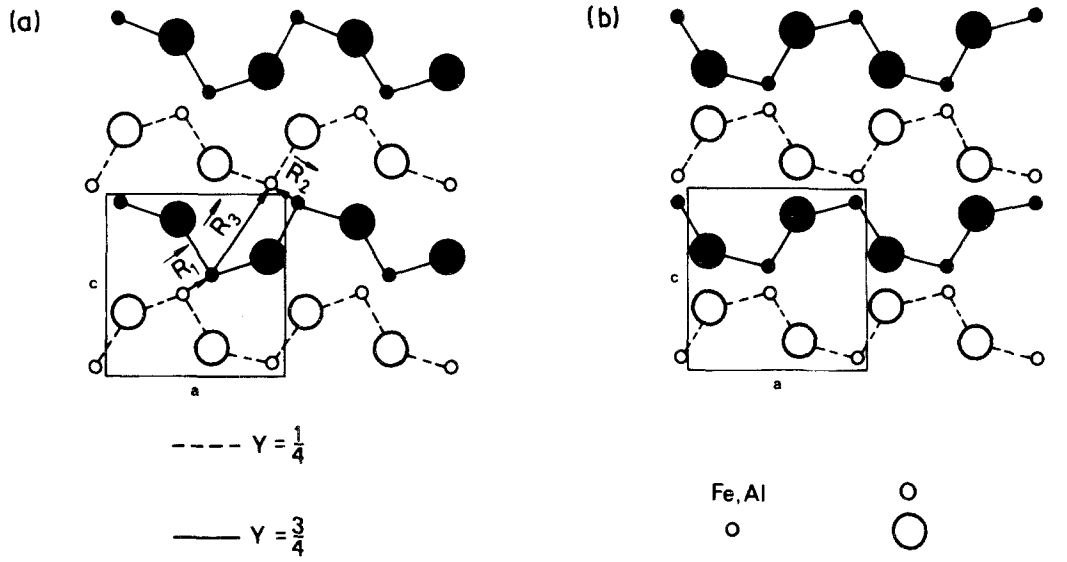

Figure 3 Arrangement of atoms in $Ca_2(Al, Fe)O_5$ at $y = \frac{1}{4}$ and $\frac{3}{4}$ for Al/Fe < 0.4(a) and Al/Fe > 0.4(b).

calcium aluminoferrite we do not deal with the simple translation faults.

When trying to interpret the TEM observations it is necessary to consider the arrangement of atoms within particular layers of calcium aluminoferrite crystal structures [2, 3, 6, 7]. The (Al, Fe)O-layers at $y = \frac{1}{4}$ and $\frac{3}{4}$ (parts of tetrahedral layers) are represented in Fig. 3 with arrangements for Al/Fe < 0.4 (a) and Al/Fe > 0.4 (b). In the arrangement belonging to Al/Fe < 0.4, the vectors between certain tetrahedral (Fe, Al) sites are comparable with the determined vectors $\mathbf{R}_1$, $\mathbf{R}_2$, and $\mathbf{R}_3$. Since the interatomic vectors for the rest of the structure do not correspond to $\mathbf{R}_1$, $\mathbf{R}_2$ and

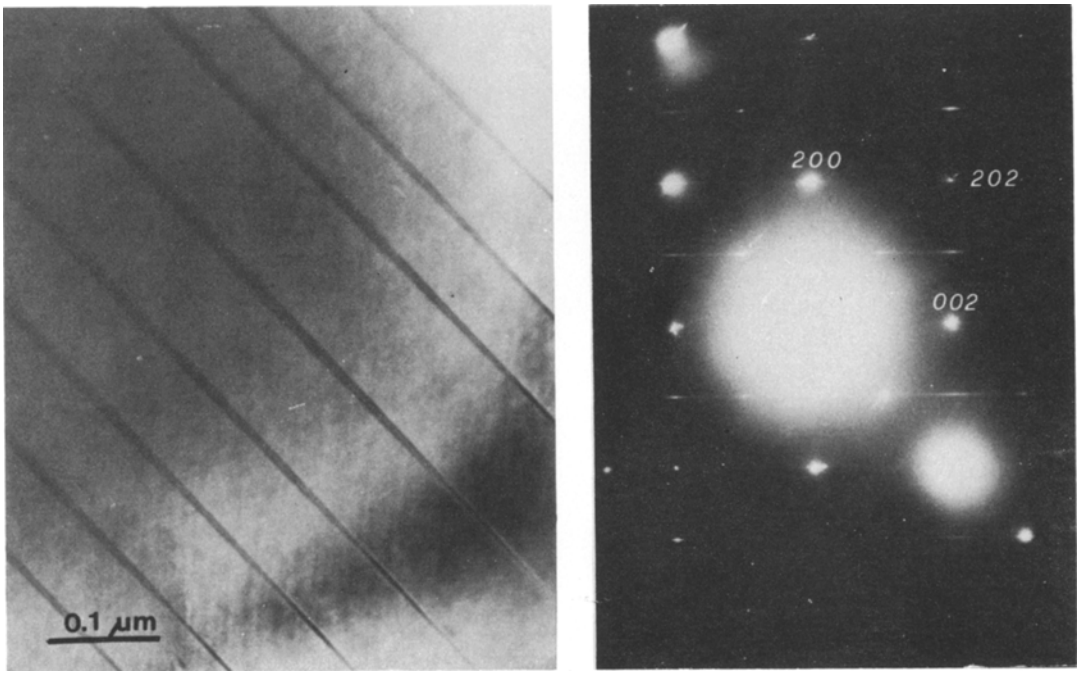

Figure 4 TEM and $h\ 0\ l$ electron diffraction pattern showing split spots.

R_3, it seems that along the observed planar interfaces a kind of chemical ordering takes place presumably in the tetrahedral layers. Such an ordering might initiate the formation of precipitates within the $Ca_2(Al, Fe, Cr)O_5$ solid solution, and some electron diffraction patterns showing split spots (Fig. 4) support this presumption. Although chemical ordering is very likely responsible for the effects observed, further work is needed to confirm the existence of the precipitates and to clarify fully the role of chromium in the formation of the observed planar interfaces.

References

1. T. SAKURAI, T. SATO and A. YOSHINAGA, "Proceedings of the 5th International Symposium on Chemistry of Cement, Tokyo, 1968", Vol. I (The Cement Association of Japan, Tokyo, 1969) p. 300.
2. E. F. BERTAUT, P. BLUM and A. SAGNIERES, *Acta Cryst.* **12** (1959) 149.
3. A. A. COLVILLE and S. GELLER, *ibid* **B27** (1971) 2311.
4. K. SMITH, *ibid* **15** (1962) 1146.
5. S. AMELINCKX and J. VAN LANDUYT, "Electron Microscopy in Mineralogy", edited by H. R. Wenk (Springer Verlag, New York, 1976) p. 68.
6. A. A. COLVILLE, *Acta Cryst.* **B26** (1970) 1469.
7. A. A. COLVILLE and S. GELLER, *ibid* **B28** (1972) 3196.

Received 26 July
and accepted 20 September 1979

I. JELENIĆ
Research Department,
Association of Yugoslav Cement Producers,
Zagreb,
Yugoslavia
A. BEZJAK
Faculty of Pharmacy and Biochemistry,
University of Zagreb,
Zagreb,
Yugoslavia
V. MARINKOVIĆ
Faculty of Natural Sciences and Technology
and Institute "Jožef Stefan".
E. Kardelj University,
Ljubljana,
Yugoslavia

Microstructural changes during large strain cyclic deformation of polypropylene

Polypropylene exhibits an excellent fatigue resistance during large strain cyclic deformation [1]. In the course of work on polypropylene deformed uniaxially beyond the gross yield point and subsequently cycled into compression, the following shape changes were observed: (a) the appearance of a neck in tension; (b) the disappearance of the neck as the specimen is compressed; (c) bulging of the specimen in the previously necked region.

The profiles of a specimen of polypropylene machined from sheets initially 1.27 cm thick to give cylindrical specimens 0.635 cm diameter and a gauge length of 1.25 cm are shown in Fig. 1.

To examine the microstructural changes occur-

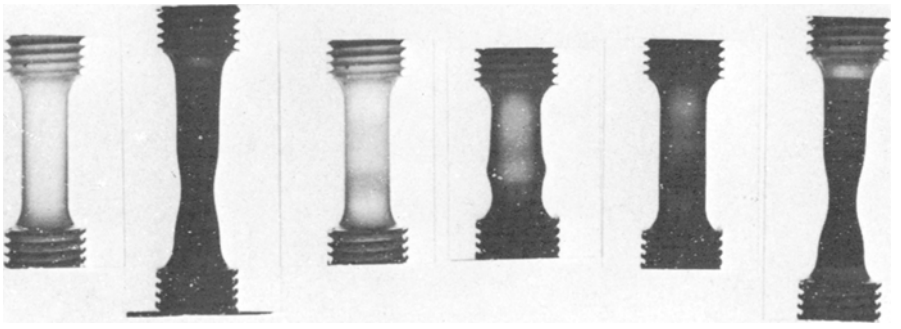

Figure 1 Unaxial cyclic deformation of polypropylene showing the microscopic shape changes which result in tension (necking) and in compression (localized bulging).

0022–2461/80/041054–04$02.40/0